

In vivo Monitoring of Organ-Selective Distribution of CdHgTe/SiO₂ Nanoparticles in Mouse Model

Haiyan Chen · Sisi Cui · Zhenzhen Tu · Yueqing Gu · Xuemei Chi

Received: 15 June 2011 / Accepted: 18 October 2011 / Published online: 3 November 2011
© Springer Science+Business Media, LLC 2011

Abstract CdHgTe/SiO₂ nanoparticles were prepared by SiO₂ capping on the surface of CdHgTe QDs. The characteristics, such as optical spectra, photostability, size and cell toxicity were investigated. The dynamic distribution of CdHgTe/SiO₂ nanoparticles was in vivo monitored by near infrared fluorescence imaging system. CdHgTe/SiO₂ nanoparticles acted as a novel fluorescence probe have a maximum fluorescence emission of 785 nm and high photo-stability. The hydrodynamic diameter of CdHgTe/SiO₂ nanoparticles could be adjusted to 122.3 nm. Compared to CdHgTe QDs, inhibitory effects of CdHgTe/SiO₂ nanoparticles on proliferation of HCT116 cells decreased to a certain extent. CdHgTe/SiO₂ nanoparticles had their specific dynamic distribution behavior, which provided new perspectives for bio-distribution of nanoparticles.

Keywords CdHgTe/SiO₂ · Nanoparticles · Organ selective · Bio-distribution · Near infrared

Introduction

Recent breakthroughs in biomedical nanotechnology have demonstrated the promising prospect of quantum dots (QDs) acting as cancer diagnostic probes [1, 2], as smart drug-delivery systems and as aids to therapy monitoring [3, 4]. QDs are featured with many unique properties, such as size-

dependent emission band spanning from UV to infrared region, high quantum yields, long effective Stokes shift and high photostability [5]. QDs of different components and surface functionalization are commercially available in recent years. Although researchers have successfully utilized various QDs fulfilling both in vitro and in vivo application, QDs containing Cd, Se, Te, Hg and Pb still have some limitations including dose-dependent cytotoxicity and degradation in physiological condition [6–8].

When toxicity of QDs continues to be investigated and debated, a numerous of experiments have demonstrated that modification of QDs' surface have a potent effect on both the QDs clearance from plasma and the sequestration of QDs within organs [9, 10]. Silica is preferred as an inert surface coating material mainly because this substance is non-toxic, stable, as well as biocompatible. Silanization of various semiconductor nanoparticles have shown outstanding superiority in protecting their surface characteristics [11, 12]. Silica coatings can preserve the encapsulated QDs from environmental factors which may affect the optical properties and stability [13]. Furthermore, silica matrix, which is easy to be modified, is suitable for conjugation to additional optical reporters or targeting groups for broader application.

Researchers have used various procedures to coating silica shells on the surface of CdTe, CdS, CdSe, CdSe/ZnS and CdSe/CdS [14–16]. The common methods used for silica coating are Stöber method and the micro-emulsion method [17]. The former one is used for nanoparticles which can be well dispersed in polar solvents such as ethanol and isopropanol, whereas the latter is suitable for hydrophobic nanoparticles. Furthermore, there are still great challenges for preparing uniform and thin silica coating on individual nanoparticles rather than on particle aggregates by far [18].

Haiyan Chen and Sisi Cui contributed equally to the work.

H. Chen · S. Cui · Z. Tu · Y. Gu (✉) · X. Chi
Department of Biomedical Engineering,
School of Life Science and Technology,
China Pharmaceutical University,
24 Tongjia Lane, Gulou District,
Nanjing 210009, China
e-mail: guyueqing@hotmail.com

Here we demonstrate controlled organ-selective biodistribution and elimination routes of nanoparticles by silica surface coating but without any specific targeting moieties. Silica coatings were modified on the surface of CdHgTe QDs. The spectral properties, size distribution and toxicity of CdHgTe/SiO₂ nanoparticles were studied. Most importantly, the dynamic behavior of CdHgTe/SiO₂ nanoparticles was *in vivo* investigated in mouse models by NIR fluorescence imaging system.

Materials

All chemicals mentioned in the current investigations were used as received; they are cadmium nitrate hydrate (Cd(NO₃)₂·4H₂O; Aldrich, 99.9%), Te powder (GuoYao chemistry agent corporation, 99.9%), sodium borohydride (NaBH₄, GuoYao chemistry agent corporation, 99%+), Thioglycolic acid (TGA, Aldrich, 97%+), (3-mercaptopropyl)-trimethoxysilane (MPS, Aladdin, 98%), sodium silicate (GuoYao chemistry agent corporation, 99.9%). Water for all reactions, solution preparation and polymer purification was double distilled. Other chemicals were of analytical grade.

Methods

Synthesis of CdHgTe/SiO₂ Nanoparticles

CdHgTe QDs was prepared following the method described previously [6]. For surface coating, 10 μl of MPS (0.2 M) solution and 3 ml of CdHgTe QDs aqueous solution were placed in a 25 mL three-neck flask. Dropwise addition of 1 M NaOH was introduced to adjust the solution to pH 11.4. Deaeration of the solution was performed under a robust flow of nitrogen with stirring at room temperature for 30 min. After vigorously stirring for 1 h at room temperature, 20 μl of sodium silicate solution (0.2 M) was added to the above solution under stirring to initiate silica polymerization on the particle surface. This shell growth was continued for 12 h in the ice bath. Next, the entire solution was placed into dialysis tubing and dialyzed versus 500 mL of basified double distilled water at pH 11 for 2 days with fresh water being changed three times each days.

Photophysical Characterization

All UV–vis spectra were recorded on a 754-PC UV–vis spectrophotometer (JingHua, China). Photoluminescence spectra were gathered on a S2000 eight-channel optical fiber spectrographotometer (Ocean Optics corporation, America) coupled with a NL-PC-2.0-763 laser ($\lambda=$

765.9 nm, nlight, China). Samples were placed in an open-sided 1-cm-path-length quartz cuvette for both UV–vis and photoluminescence measurements.

To exam the photostabilities of the CdHgTe QDs encapsulated in silica particles, the composite particles and CdHgTe QDs in plasma medium were subjected to a continuum irradiation (765 nm) with a light intensity of 36 mW at a focus where the light beam was 1 cm in diameter. The aqueous dispersions of various particle samples were aerated with oxygen before they were transferred into a 1 cm quartz corvette for the photo-oxidation experiments.

Size Characterization of CdHgTe/SiO₂ Nanoparticles

The hydrodynamic diameter and polydispersity index (PDI) of CdHgTe/SiO₂ nanoparticles were characterized with the aid of Mastersizer 2000 Laser Particle Size Analyzer (Malvern, British) at 25 °C. A helium-neon laser (10 mW max, Wand wavelength of 633 nm) was used as the light source. P.I. was utilized to evaluate the distribution of nanoparticles population.

Cytotoxicity Studies of CdHgTe/SiO₂ Nanoparticles

To evaluate the biocompatibility of CdHgTe/SiO₂ nanoparticles as imaging probes, the cytotoxicity of CdHgTe/SiO₂ nanoparticles and CdHgTe QDs was investigated by using the MTT assay. Briefly, HCT116 cells (Human colorectal cancer cells) were seeded in a 96-well plate at a density of 5,000 cells/well on the day before the addition of the nanoparticles. CdHgTe/SiO₂ nanoparticles and CdHgTe QDs were incubated with cells in HCT116 cell culture medium in a cell culture incubator. The survival rates of HCT116 cells at 36 h after conjugates incubation were measured by MTT assay. After 3 h incubation at 37 °C, the MTT working solution was removed. Then 200 μL DMSO was added into each well and the plate was shaken for 20 min at room temperature. All samples were assayed in triplicate and the survival rate was calculated as follows: Survival rate=(mean absorbance of test wells-mean absorbance of medium control well)/(mean absorbance of untreated wells-mean absorbance of medium control well)×100%.

Dynamic Distribution of CdHgTe/SiO₂ Nanoparticles in Mouse Model

Kunmin mice, 6–8 weeks old and about 20 g in weight, were provided by China Pharmaceutical experiment animal center. All experiments were carried out in compliance with the guide for the care and use of laboratory animals in China Pharmaceutical University. The Kunmin mice were denuded by a mixture of Na₂S (5%) and starch followed

immediately by daubing camphor ice to avoid further skin erosion. The denuded mice were put back into the animal house for 24 h before experiment.

Each mouse was anesthetized with 150 μL ethyl carbamate (20 mg/mL) by intraperitoneal (IP) injection and fixed in the Lucite jig. 100 μL of CdHgTe/SiO₂ aqueous solution (8 $\mu\text{mol/L}$) was then injected into the tail vein. The dynamic behaviors of CdHgTe/SiO₂ nanoparticles were detected by near infrared (NIR) fluorescence imaging system (A high sensitive NIR CCD camera (Princeton, America), an 800 nm long pass filter (Chroma, Rockingham, VT), a NL-PC-2.0-763 laser ($\lambda=765.9$ nm, nlight, China) and HLU32F400 808 nm laser (LIMO, Dortmund, Germany)). The background image was obtained before CdHgTe/SiO₂ nanoparticles injection. A series of images was gathered at different time point (5 min, 1 h, 3 h, 8 h, 12 h and 36 h) post-injection. The mouse was executed 2 days after injection of CdHgTe/SiO₂ nanoparticles. Fluorescence images were collected after performing a thoracotomy on the executed mouse. The major organs of the mouse (liver, lungs, intestines and heart) were separated after thoracotomy and washed by normal saline. The isolated organs were put together to collect fluorescence signals by NIR image system.

Results

Synthesis of CdHgTe/SiO₂ Nanoparticles

Herein, we report on a method for preparation CdHgTe QDs coated with silica at room temperature. The synthesis routine of CdHgTe/SiO₂ nanoparticles is shown in Fig. 1. Recently, wang et al. [2] has synthesized CdTe QDs embedded silica nanoparticles by microemulsion method. However, the PL emission of CdTe QDs was severely decreased before adding poly (dimethyldiallyl ammonium chloride). In comparison, our synthetic process is straightforward without introducing extra materials besides MPS and sodium silicate. The fluorescence intensity of CdHgTe/SiO₂ nanoparticles have no seriously affect by silica shell.

Unlike commonly used methods such as microemulsion methods, this synthesis routine is both simple and practical which could also avoid using the potential toxic organic solvents.

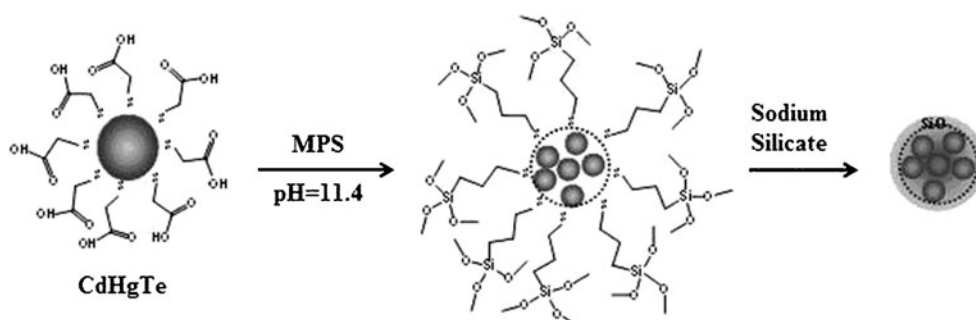
Absorbance and Fluorescence Spectra of CdHgTe/SiO₂ Nanoparticles

The absorption and emission spectra of CdHgTe/SiO₂ nanoparticles and CdHgTe QDs in water are shown in Fig. 2(a and b). The UV–vis absorption spectrum shows the characteristic electron–hole pair peak representative of the band gap energy. The shoulder peak position (720 nm) shows no significant change as SiO₂ capping on the surface of the QDs. Compared with CdHgTe QDs, the emission spectra show that CdHgTe/SiO₂ nanoparticles hold the same peak emission wavelength (790 nm) but the weaker fluorescence intensity. In this study, we obtained CdHgTe/SiO₂ nanoparticles through optimizing synthesis conditions, including addition quantity of MPS and pH adjustment. CdHgTe/SiO₂ nanoparticles with high fluorescence intensity were prepared by controlling pH at 10.5 to 11.0, using sodium silicate solution (0.2 M) to initiate silica polymerization on the surface of CdHgTe QDs. Comparison to CdHgTe QDs, the fluorescent peak position of CdHgTe/SiO₂ nanoparticles was nearly invariant with more narrow full width at half-maximum (FWHM). As shown in Fig. 2b, the quantum yield of CdHgTe QDs was 18% referring to Rhodamine 6 G, the quantum yield of CdHgTe/SiO₂ nanoparticles was approximately 16%.

Photostability of CdHgTe/SiO₂ Nanoparticles

Figure 3 shows the photostability of CdHgTe/SiO₂ nanoparticles and CdHgTe QDs in plasma medium under continuous irradiation with a 765 nm laser light. Compared to CdHgTe QDs, the fluorescence intensity of CdHgTe/SiO₂ nanoparticles almost remained the same as the original value when the laser irradiated for 120 min, which suggested excellent stability of CdHgTe/SiO₂ in a biological environment.

Fig. 1 Synthesis routine of CdHgTe/SiO₂ nanoparticles



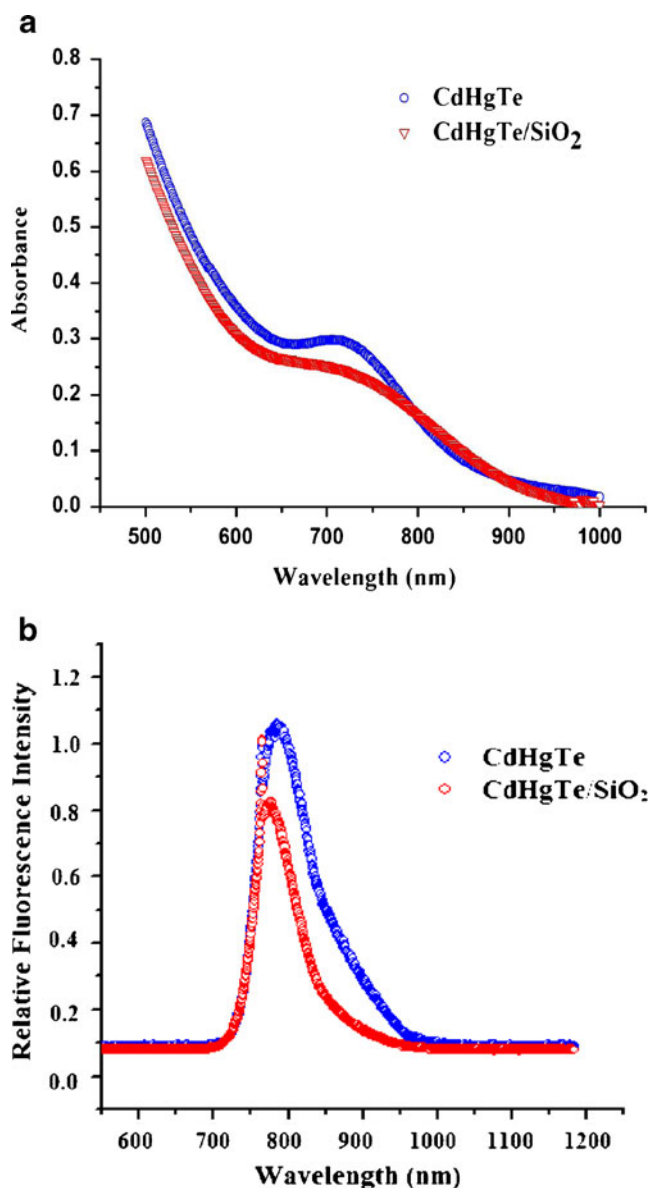


Fig. 2 **a** Absorbance spectra of CdHgTe QDs and CdHgTe/SiO₂ nanoparticles; **b** fluorescence spectra of CdHgTe QDs and CdHgTe/SiO₂ nanoparticles

Size Distribution of CdHgTe/SiO₂ Nanoparticles

As shown in Fig. 4, the size of CdHgTe/SiO₂ nanoparticles prepared with 10 μ L of MPS (0.2 M) and 20 μ L of sodium silicate (0.2 M) are 122.3 ± 38.6 nm. The nanoparticles also show narrow distribution with a relative standard deviation of 15%. The narrow size distribution of CdHgTe/SiO₂ nanoparticles indicated the synthesis of uniform nanoparticles.

Cytotoxicity of CdHgTe/SiO₂ Nanoparticles

To evaluate the biocompatibility of CdHgTe/SiO₂ nanoparticles as imaging probes, the cytotoxicity of CdHgTe/

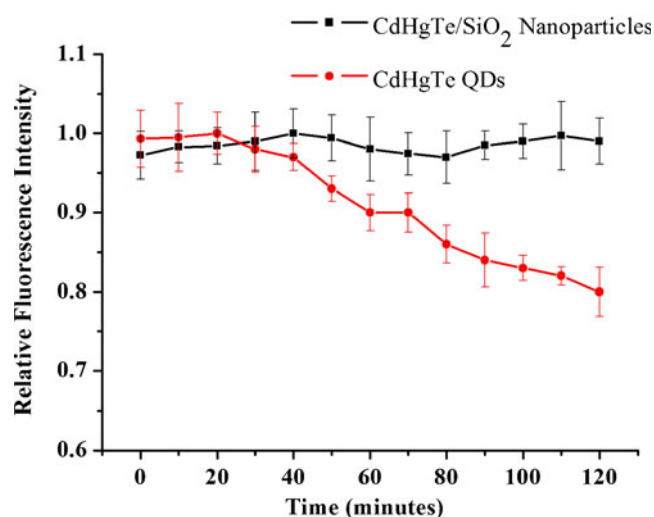


Fig. 3 Photostability of CdHgTe/SiO₂ nanoparticles and CdHgTe QDs in plasma medium under continuous irradiation by 765 nm laser for 120 min

SiO₂ nanoparticles and CdHgTe QDs are investigated by using the MTT assay. Figure 5 demonstrates a dose independence of MTT absorbance for cells being treated with CdHgTe/SiO₂ nanoparticles. After having been incubated for 36 h, CdHgTe/SiO₂ nanoparticles display very low toxicity (cell viability as high as 90%) to HCT116 cells even at higher dose. However, CdHgTe QDs exhibit cytotoxicity towards HCT116 cells at high dose (14 mM) and cause a significant reduction (about 75% of control) in cell viability. Meanwhile, an evident reduction in cell viability (about 30% of control) was also observed even when tested at the low concentration (14 μ M).

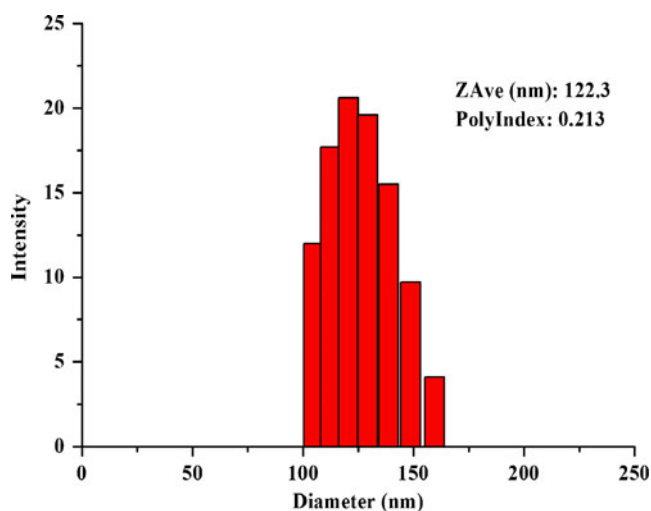


Fig. 4 Size distribution of the CdHgTe/SiO₂ nanoparticles prepared with 10 μ L MPS and 20 μ L sodium silicate (0.2 M)

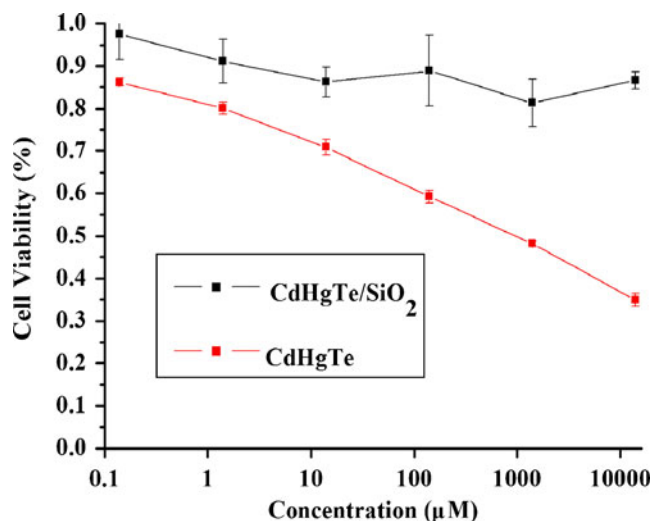


Fig. 5 Cytotoxicity studies of HCT116 cells treated with CdHgTe/SiO₂ nanoparticles and CdHgTe QDs. MTT assays illustrating cell viability upon exposing the cells with different concentration of CdHgTe/SiO₂ nanoparticles and CdHgTe QDs for 36 h

Dynamic Characteristics of CdHgTe/SiO₂ Nanoparticles In vivo

The in vivo dynamic behavior of CdHgTe/SiO₂ nanoparticles (122.3±38.6 nm) is investigated in mouse model by NIR fluorescence imaging system. A series of fluorescent images are displayed in Fig. 6, which were taken at different time interval after injection of CdHgTe/SiO₂ nanoparticles. The fluorescent background was acquired prior to CdHgTe/SiO₂ nanoparticles injection (Fig. 6a). After injection, fluorescence images were collected at different time points (10s, 5 min, 1 h, 3 h, 8 h, 12 h, 36 h). As shown in Fig. 6b, CdHgTe/SiO₂ nanoparticles quickly distributed in the blood vessels of the whole body via blood circulation and accumulated quickly in heart. For a short while, fluorescence signals could be distinctly acquired in lung and liver of the mouse (Fig. 6c). The fluorescence signals of high intensity in lung maintained within 36 h post-injection (Fig. 6d to h). It is worth noting that these results are helpful for localizing and monitoring diseases of liver and lungs. Owing to the clearance of CdHgTe/SiO₂ nanoparticles, fluorescence intensity in liver obviously decreased at 36 h post-injection. Whereas, fluorescence signals of lung remained at high level. The mouse was executed and performed a thoracotomy at 1 h and 48 h, respectively. Fluorescence signals of mouse liver and lungs could still be clearly distinguished (Fig. 6i and j). The major organs of the mouse were isolated and put together to collect fluorescence images. In comparison with other organs, fluorescence signals in lungs were the most obvious (Fig. 6k). The results demonstrate that lung is the primary target organ for CdHgTe/SiO₂ nanoparticles (122.3±38.6 nm) to accumulate in mouse model.

Discussion

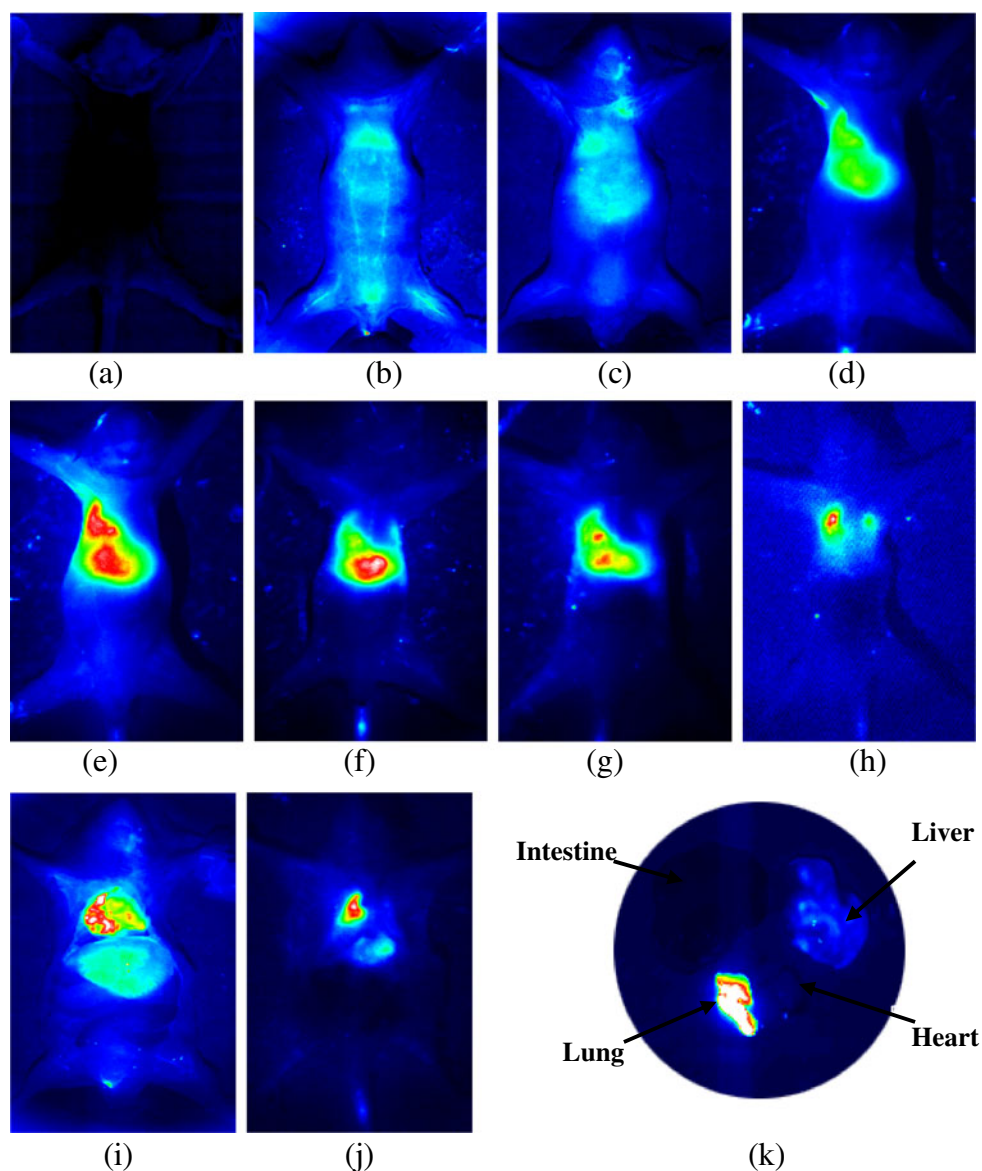
In order to obtain CdHgTe/SiO₂ nanoparticles with high PL efficiency, synthetic conditions should be strictly controlled especially pH condition. Researchers found out that silanization of TGA stabilized CdTe QDs began with the ligand exchange of TGA with MPS molecules [19]. MPS carries negative charges at alkaline pH. CdHgTe QDs can be stabilized by TGA at alkaline pH as well. It is due to the fact that polymerization of the silica must be performed at high pH to active sodium silicate. Hence, we prepared CdHgTe/SiO₂ nanoparticle at pH 11 to advance the removal of TGA off the surface and priming of MPS onto the surface of CdHgTe QDs.

The photoluminescence efficiency almost retains the initial efficiency even capping with SiO₂ shell. The reasons for the high efficiency are attributed to the proper pH controlling during incorporation of the QDs and the high concentration of QDs capping with a thin silica layer without removing ligands (TGA). To obtain high fluorescence intensity of CdHgTe/SiO₂ nanoparticles, it is important to retain the stability of the QDs during incorporation. TGA stabilized CdHgTe QDs in aqueous solution exhibits high fluorescence intensity in the pH range of 8–11 because carboxyl groups in TGA molecules have a dissociated form in such alkaline conditions. Deionization of TGA increases greatly when pH changed from 2.9 to 4.9, which destroys the interaction between thiol group and CdHgTe QDs and makes the QDs unstable and promotes the agglomeration [20]. As a result, in the preparation of CdHgTe/SiO₂ nanoparticles, alkaline solution with pH 8–10 was used during the Stöber synthesis. Meanwhile, optimization of the addition quantity of MPS also benefits the optical properties of CdHgTe/SiO₂ nanoparticles, which is prominently correlative with the thickness of silica shell grown on CdHgTe QDs surface. Furthermore, no addition of organic solvents during incorporation results in high photoluminescence efficiency because organic solvents results in aggregation and precipitation of the QDs.

The CdHgTe/SiO₂ nanoparticles in aqueous solution show excellent stability in vitro. No particles aggregation was observed in the exposure of atmosphere and light within several weeks. Although the surface ligands of QDs are susceptible to environmental factors, silica coating can effectively prevent QDs from oxidizing and aggregating. After silylation, the passivation of the CdHgTe QDs surface enhances the stability of CdHgTe QDs in aqueous solution.

In comparison with the size of CdHgTe QDs precursor, it is obvious that multiple QDs rather than only one QD are embedded into silica shell which benefits the fluorescent intensity of CdHgTe/SiO₂ nanoparticles. We found that the amount of added sodium silicate influence the size of the

Fig. 6 The dynamic biodistribution of CdHgTe/SiO₂ nanoparticles (122.3±38.6 nm) were monitored after tail vein injection of CdHgTe/SiO₂ nanoparticles into the mice. **a** the fluorescence background obtained before injection (excitation at 765 nm); Fluorescence images of the mouse at different time interval: **b** 5 min; **c** 1 h; **d** 3 h; **e** 8 h; **f** 12 h; **g** 24 h; **h** 36 h; **i** and **j** the mouse was put into execution 1 hour later and 2 days later, and then fluorescence image of the mouse was taken after performing a thoracotomy, respectively; **k** fluorescence image of isolated tissues after mouse execution (heart, lung, liver and intestines)



resulting nanoparticles. While 10 μL of sodium silicate (0.2 M) rather than 20 μL were added into the reactive solution, CdHgTe/SiO₂ nanoparticles with the size of 22.8 ± 5.2 nm could be obtained (data were not shown). Meanwhile, larger CdHgTe/SiO₂ nanoparticles with multiple QDs inside can be prepared by increasing the amount of sodium silicate. Therefore, the quantity of sodium silicate is the main factor that determines the size distribution of CdHgTe/SiO₂ nanoparticles.

In recent years, QDs have attracted enormous attention for their applications in biological and medical areas. However, their potential toxicity and stability are the most highly debated issues concerning the application of QDs especially for in vivo bio-imaging. The potential toxicity associated with their application in living body mainly arises from the inherent chemical composition like heavy metals. The heavy metals can easily accumulate in adipose

tissues which are unable to be excreted out of the body more than one decade [21]. Surface oxidation of QDs induced by air or ultraviolet rays is correlated with the cototoxicity of QDs, which lead to liberation of free heavy metal ions [22]. To modulate the toxicity of QDs in vivo, the dosage should be taken into consideration while using QDs in living animals. As mentioned in detail, the maximum safe dose of CdHgTe QDs used in mice is 10.5 $\mu\text{g/g}$ [6]. In this study, the maximum safe dose of CdHgTe/SiO₂ nanoparticles in mouse model is 85.0 $\mu\text{g/g}$ (data did not shown), which is much higher than that of CdHgTe QDs. The results indicate that the innocuous silica shells can prevent QDs from oxidation and avoid releasing heavy metal ions effectively. Meanwhile, the silica shell can enhance the stability of CdHgTe QDs to resist hostile environment. In addition, our synthetic method is a green route which avoids utilizing the potential toxic materials.

Therefore, CdHgTe/SiO₂ nanoparticles are safe for in vivo usage and their fluorescence intensity is sufficient enough for in vivo imaging at our injection dose.

The primary purpose of our study is to improve the biocompatibility and stability of CdHgTe QDs as well as weakened the toxicity of CdHgTe QDs for in vivo application. Silica, amphiphilic and functionalized lipids, have been used as surface coating matrix due to their excellent properties, for instance their good stability, the ability to be modified and favorable biocompatibility. It is of importance to control the surface properties of QDs because it will determine their fate in living bodies. In our study, the fluorescence intensity of CdHgTe/SiO₂ nanoparticles in vivo during bioimaging is as excellent as their PL intensity in vitro, demonstrating that silica coating has less impact on the fluorescence intensity of the QDs.

QDs were regarded as excellent extrinsic contrast agents for in vivo imaging compared to the commonly used organic dyes. Investigating the accumulation and distribution kinetics of QDs in vivo is crucial for biomedical applications in order to improve the sensitivity and selectivity of bioimaging outcome. Commonly, QDs are primarily accumulated in the liver after intravenous injection into the body. This phenomenon relates to the nonspecific uptake of QDs by the reticuloendothelial system (RES) mainly located in the liver, lymph nodes, bone marrow and spleen. If QDs enter the body via subcutaneous injection, nonspecific uptake of QDs by RES was not as severe as intravenous injection, but it could also be confirmed by inductively coupled plasma mass spectrometry (ICP-MS) [19]. Although NIR fluorescence imaging is unable to provide quantitative information of the QDs like ICP-MS, the kinetics of QDs could be directly observed in vivo by means of monitoring the fluorescent signals. We have previously investigated in vivo dynamic characteristics of thiol-stabilized CdHgTe QDs. The QDs rapidly accumulated in mouse liver and then enter into intestine via hepato-enteric circulation. In this study, CdHgTe/SiO₂ nanoparticles without further functionalization showed pronounced nonspecific tissue binding as well, which is similar to the bare QDs. Nevertheless, we found that CdHgTe/SiO₂ nanoparticles accumulated in large quantities in lung other than in liver. The fluorescence images of the isolated organs provide definite evidence that the lungs are the major targeted organs of CdHgTe/SiO₂ nanoparticles.

The different dynamic properties between CdHgTe QDs and CdHgTe/SiO₂ nanoparticles are attributed to different size between CdHgTe/SiO₂ nanoparticles (122 nm) and CdHgTe QDs (5–7 nm). The size of non-functionalized QDs is a predominant factor that leads to difference of their in vivo dynamic properties [23]. De Jong et al. have found that Particle size-dependent organ distribution of gold

nanoparticles after intravenous administration. Particles of 10 nm were present in various organ systems whereas the larger particles were only detected in blood, liver and spleen [24]. Chithran et al. also showed the size and shape dependence of gold nanoparticle uptake into mammalian cells [9]. Furthermore, due to the phagocytosis of alveolar macrophages, larger particles (>100 nm) are prone to being phagocytized in lungs. The lung-targeting of CdHgTe/SiO₂ nanoparticles may provide a promising prospect for the non-invasive monitoring of lung related studies.

Conclusion

CdHgTe/SiO₂ nanoparticles with excellent photophysical properties were synthesized in water phase. These nanoparticles with NIR fluorescence and super photo-stability are well appropriate for in vivo dynamic studies. Their biodistribution in mouse model revealed that the size is a predominant factor on influencing organ-selective behaviors. For broader application in tumor diagnosis studies, CdHgTe/SiO₂ nanoparticles should be further functionalized with additional targeting moieties on their surfaces. In future, exploiting NIR photoluminescence CdHgTe/SiO₂ nanoparticles can provide an outstanding candidate for low toxic bio-imaging, which has great significance for the guidance of site-directed surgeries as well as disease diagnosis and therapy.

Acknowledgement The authors are grateful to Natural Science Foundation Committee of China (NSFC 81000666, NSFC30700779, NSFC30800257, NSFC31050110123 and NSFC81071194), China Pharmaceutical University (JKQ2009004), the Ministry of Science and Technology (2009ZX09310-004) for their financial supports.

References

1. Tisdale WA, Zhu XY (2011) Surface chemistry special feature: artificial atoms on semiconductor surfaces. *Proc Natl Acad Sci U S A* 108(3):965–970
2. Wang C, Ma Q, Dou W, Kanwal S, Wang G, Yuan P, Su X (2009) Synthesis of aqueous CdTe quantum dots embedded silica nanoparticles and their applications as fluorescence probes. *Talanta* 77(4):1358–1364
3. Boeneman K, Deschamps JR, Buckhout-White S, Prasuhn DE, Blanco-Canosa JB, Dawson PE, Stewart MH, Susumu K, Goldman ER, Ancona M, Medintz IL (2010) Quantum dot DNA bioconjugates: attachment chemistry strongly influences the resulting composite architecture. *ACS Nano* 4(12):7253–7266
4. Fichter KM, Flajolet M, Greengard P, Vu TQ (2010) Kinetics of G-protein-coupled receptor endosomal trafficking pathways revealed by single quantum dots. *Proc Natl Acad Sci U S A* 107(43):18658–18663
5. Maldiney T, Richard C, Seguin J, Wattier N, Bessodes M, Scherman D (2011) Effect of core diameter, surface coating, and

- PEG chain length on the biodistribution of persistent luminescence nanoparticles in mice. *ACS Nano* 5(2):854–862
6. Chen H, Wang Y, Xu J, Ji J, Zhang J, Hu Y, Gu Y (2008) Non-invasive near infrared fluorescence imaging of CdHgTe quantum dots in mouse model. *J Fluoresc* 18(5):801–811
 7. Mahto SK, Park C, Yoon TH, Rhee SW (2010) Assessment of cytocompatibility of surface-modified CdSe/ZnSe quantum dots for BALB/3 T3 fibroblast cells. *Toxicol In Vitro* 24(4):1070–1077
 8. Wang L, Zhang J, Zheng Y, Yang J, Zhang Q, Zhu X (2010) Bioeffects of CdTe quantum dots on human umbilical vein endothelial cells. *J Nanosci Nanotechnol* 10:8591–8596
 9. Chithrani BD, Ghazani AA, Chan WC (2006) Determining the size and shape dependence of gold nanoparticle uptake into mammalian cells. *Nano Lett* 6(4):662–668
 10. Fischer HC, Liu L, Pang KS, Chan WCW (2006) Pharmacokinetics of nanoscale quantum dots: in vivo distribution, sequestration, and clearance in the rat. *Adv Funct Mater* 16(10):1299–1305
 11. Buiculescu R, Hatzimarinaki M, Chaniotakis NA (2010) Biosilicated CdSe/ZnS quantum dots as photoluminescent transducers for acetylcholinesterase-based biosensors. *Anal Bioanal Chem* 398(7–8):3015–3021
 12. Cherkouk C, Rebohle L, Skorupa W (2011) Bioconjugation of the estrogen receptor hER α to a quantum dot dye for a controlled immobilization on a SiO₂ surface. *J Colloid Interface Sci* 355(2):442–447
 13. Hu X, Gao X (2010) Silica-polymer dual layer-encapsulated quantum dots with remarkable stability. *ACS Nano* 4(10):6080–6086
 14. Darbandi M, Urban G, Krüger MA (2010) Facile synthesis method to silica coated CdSe/ZnS nanocomposites with tuneable size and optical properties. *J Colloid Interface Sci* 351(1):30–34
 15. Jie GF, Liu P, Zhang SS (2010) Highly enhanced electrochemiluminescence of novel gold/silica/CdSe-CdS nanostructures for ultrasensitive immunoassay of protein tumor marker. *Chem, Commun (Camb)* 46(8):1323–1325
 16. Ren T, Erker W, Basché T, Schärfl W (2010) Synthesis and spectroscopic properties of silica-dye-semiconductor nanocrystal hybrid particles. *Langmuir* 26(23):17981–17988
 17. Hu X, Zrazhevskiy P, Gao X (2009) Encapsulation of single quantum dots with mesoporous silica. *Ann Biomed Eng* 37(10):1960–1966
 18. Selvan ST, Tan TT, Ying JY (2005) Robust, non-cytotoxic, silica-coated cdse quantum dots with efficient photoluminescence. *Adv Mater* 17(13):1620–1625
 19. Pic E, Pons T, Bezdtnaya L, Leroux A, Guillemin F, Dubertret B, Marchal F (2010) Fluorescence imaging and whole-body biodistribution of near-infrared-emitting quantum dots after subcutaneous injection for regional lymph node mapping in mice. *Mol Imaging Biol* 12(4):394–405
 20. Dezhurov SV, Volkova IY, Wakstein MS (2011) FRET-based biosensor for oleic acid in nanomolar range with quantum dots as an energy donor. *Bioconjug Chem* 22(3):338–345
 21. Medintz IL, Mattoussi H, Clapp AR (2006) Potential clinical application of QDs. *Int J Nanomed* 3(2):151–167
 22. Mancini MC, Kairdolf BA, Smith AM, Nie S (2008) Oxidative quenching and degradation of polymer-encapsulated quantum dots: new insights into the long-term fate and toxicity of nanocrystals in vivo. *J Am Chem Soc* 130(33):10836–10837
 23. Choi HS, Ipe BI, Misra P, Lee JH, Bawendi MG, Frangioni JV (2009) Tissue- and organ-selective biodistribution of NIR fluorescent quantum dots. *Nano Lett* 9(6):2354–2359
 24. De Jong WH, Hagens WI, Krystek P, Burger MC, Sips AJ, Geertsma RE (2008) Particle size-dependent organ distribution of gold nanoparticles after intravenous administration. *Biomaterials* 29(12):1912–1919